
10-30-2017

Predicting Dry-Season Flows with a Monthly Rainfall–Runoff Model: Performance for Gauged and Ungauged Catchments

Perrine Hamel
Stanford University

Andrew John Guswa
Smith College, aguswa@smith.edu

Jake Sahl
Stanford University

Lu Zhang
CSIRO Land and Water

Follow this and additional works at: https://scholarworks.smith.edu/egr_facpubs



Part of the [Engineering Commons](#)

Recommended Citation

Hamel, Perrine; Guswa, Andrew John; Sahl, Jake; and Zhang, Lu, "Predicting Dry-Season Flows with a Monthly Rainfall–Runoff Model: Performance for Gauged and Ungauged Catchments" (2017). Engineering: Faculty Publications, Smith College, Northampton, MA.
https://scholarworks.smith.edu/egr_facpubs/16

This Article has been accepted for inclusion in Engineering: Faculty Publications by an authorized administrator of Smith ScholarWorks. For more information, please contact scholarworks@smith.edu

Predicting dry-season flows with a monthly rainfall-runoff model: performance for gauged and ungauged catchments

Journal:	<i>Hydrological Processes</i>
Manuscript ID	HYP-16-0717.R2
Wiley - Manuscript type:	Research Article
Date Submitted by the Author:	11-Jul-2017
Complete List of Authors:	Hamel, Perrine; Stanford University Woods Institute for the Environment, Natural Capital Project Guswa, Andrew; Smith College, Picker Engineering Program Sahl, Jake; Stanford University Woods Institute for the Environment, Natural Capital Project Zhang, Lu; CSIRO Land and Water, Christian Laboratory
Keywords:	baseflow, land-use change, climate change, DWBM, prediction in ungauged basins

SCHOLARONE™
Manuscripts

Review

1
2
3 1 Predicting dry-season flows with a monthly rainfall-runoff model:
4
5
6 2 performance for gauged and ungauged catchments
7
8
9
10 3

11
12 4 Perrine Hamel^{*a}, Andrew Guswa^{b,a}, Jake Sahl^a, Lu Zhang^c
13
14
15 5

16
17 6 ^a Natural Capital Project, Woods Institute for the Environment, Stanford University.
18 7 371 Serra Mall, Stanford, CA 94305, USA. ph: +1 650-725-1783
19 8 perrine.hamel@stanford.edu; jakesahl@gmail.com
20

21 9 ^b Picker Engineering Program, Smith College, Northampton, MA 01063. aguswa@smith.edu
22

23 10 ^c CSIRO Land and Water, GPO Box 1666, Canberra ACT 2601, Australia. lu.zhang@csiro.au
24
25
26 11

27
28 12 * Corresponding author
29
30
31
32
33
34
35
36
37
38
39
40
41
42
43
44
45
46
47
48
49
50
51
52
53
54
55
56
57
58
59
60

1
2
3 13 **Abstract**
4
5

6 14 Hydrologic models are useful to understand the effects of climate and land-use changes on dry-
7
8 15 season flows. In practice, there is often a trade-off between simplicity and accuracy, especially
9
10 16 when resources for catchment management are scarce. Here, we evaluated the performance of
11
12 17 a monthly rainfall-runoff model (dynamic water balance model, DWBM) for dry-season flow
13
14 18 prediction under climate and land-use change. Using different methods with decreasing
15
16 19 amounts of catchment information to set the four model parameters, we predicted dry-season
17
18 20 flow for 89 Australian catchments, and verified model performance with an independent dataset
19
20 21 of 641 catchments in the United States. For the Australian catchments, model performance
21
22 22 without catchment information (other than climate forcing) was fair; it increased significantly as
23
24 23 the information to infer the four model parameters increased. Regressions to infer model
25
26 24 parameters from catchment characteristics did not hold for catchments in the United States,
27
28 25 meaning that a new calibration effort was needed to increase model performance there.
29
30 26 Recognizing the interest in relative change for practical applications, we also examined how
31
32 27 DWBM could be used to simulate a change in dry-season flow following land-use change. We
33
34 28 compared results with and without calibration data, and showed that predictions of changes in
35
36 29 dry-season flow were robust with respect to uncertainty in model parameters. Our analyses
37
38 30 confirm that climate is a strong driver of dry-season flow and that parsimonious models such as
39
40 31 DWBM have useful management applications: predicting seasonal flow under various climate
41
42 32 forcings when calibration data are available, and providing estimates of the relative effect of
43
44 33 land-use on seasonal flow for ungauged catchments.
45
46
47
48
49

50 34 **Keywords:** baseflow; land-use change; climate change; DWBM; prediction for ungauged basins
51
52
53
54 35
55
56
57
58
59
60

36 1 Introduction

37 With increasing pressure on water resources globally, managers of water resources need to
38 understand how streamflows – in particular, dry-season flows – respond to changes in land use
39 and climate. Applications vary broadly: at the global scale, hydrologists aim to better predict the
40 effect of agricultural expansion on water resources to avoid additional pressure in water-scarce
41 regions (Brauman et al., 2016). At the regional scale, water resources assessments are needed
42 to explore and implement efficient water-allocation plans (Kirby et al., 2014). For example, the
43 development of hydropower production facilities in Africa or South-East Asia requires the
44 prediction of annual and monthly flows (Vogl et al., 2016). In Latin America, the development of
45 investment in watershed services programs requires stakeholders to estimate the effect of land
46 management on hydrological services (Bremer et al., 2016; Guswa et al. 2014).

47 A number of knowledge gaps hinder the development of decision-aid tools for water resources
48 management. First, the effects of environmental changes on baseflow remain uncertain
49 (Andréassian, 2004; Brown et al., 2013, 2005; Price, 2011). Here, we define baseflow as
50 “streamflow fed from deep subsurface and delayed shallow subsurface storage between
51 precipitation and/or snowmelt events” (Price, 2011). Baseflow depends on many factors: climate
52 (magnitude and seasonality of precipitation and evapotranspiration), topography, geology, and
53 land use and land cover – with vegetation type and age as key subfactors (Brutsaert, 2008; Gao
54 et al., 2015; Zhang et al., 2014). In addition, the relative importance of these factors vary in time,
55 at the event and seasonal time scales (Devito et al., 2005; Jencso and McGlynn, 2011), making
56 it difficult to characterize in a given location. Second, relatedly, hydrologic models are limited in
57 their ability to estimate dry-season flow: lumped models tend to oversimplify the complexity of
58 hydrological processes, which casts doubt on their capacity to predict the effect of land use or
59 climate change. Complex models have high-data needs, require calibration, and often show

1
2
3 60 high uncertainty for predictions outside of the calibration conditions (in particular under land-use
4
5 61 change) (McIntyre et al., 2014; Smith et al., 2004).
6
7

8
9 62 Recognizing and seeking to fill these knowledge gaps is important, and taking stock of current
10
11 63 knowledge and its usefulness for practical applications is of equal priority for management. By
12
13 64 identifying questions that are of interest for water-resources management, hydrologists can
14
15 65 better understand where research gaps need to be filled. Typically, answering landscape
16
17 66 management questions requires an understanding of: i) the absolute magnitude of the *change*
18
19 67 in dry-season flow following land-use or climate change; ii) the relative difference in dry-season
20
21 68 flows among various land uses or management scenarios (e.g. afforestation, deforestation,
22
23 69 water abstraction for domestic or agricultural use); and iii) the spatial distribution of contributions
24
25 70 to baseflow (i.e. whether some part of the landscapes provide more baseflow than others)
26
27
28 71 (Guswa et al., 2014).
29
30

31 72 This paper explores the first two questions by analyzing how a simple monthly rainfall-runoff
32
33 73 model can capture major drivers of dry-season flow. Our aim is to quantify predictive uncertainty
34
35 74 in dry-season flow across a wide range of climate and catchment characteristics, and to assess
36
37 75 how this uncertainty changes as catchment information is introduced. In an era of increasingly
38
39 76 available data, in particular global daily precipitation data (Gehne et al., 2016), our work at the
40
41 77 monthly time step is justified by the parsimony of models operating at this time scale (Mouehli et
42
43 78 al., 2006). This characteristic facilitates regionalization and work in ungauged basins (Perrin et
44
45 79 al., 2001), as well as any analysis that does not necessitate short time-scale representation of
46
47 80 the flow regime: e.g., optimization approaches for reservoir operation or irrigation schemes
48
49 81 (Hughes, 2004; Kirby et al., 2014), or drought assessment (Smakhtin and Hughes, 2007). In
50
51 82 both circumstances, quantifying the uncertainty of uncalibrated models is important to produce
52
53 83 credible information for management, potentially overcoming the need for more sophisticated
54
55 84 models (Guswa et al., 2014).
56
57
58
59
60

1
2
3 85 Here, we used DWBM (dynamic water balance model) with a monthly time step (Zhang et al.
4
5 86 2008). The model has four parameters with physical interpretation and was shown to explain
6
7 87 flow variations for a large number of catchments in Australia (Zhang et al., 2016, 2008). After
8
9 88 describing the model and how climate influences its behavior, we examine the correlations
10
11 89 between catchment characteristics and calibrated model parameters. We examine how model
12
13 90 parameters are correlated with physical characteristics, and show that model performance for
14
15 91 dry-season flow prediction decreases sharply when catchment information is reduced. We also
16
17 92 examine predicted change in dry-season flow following a simulated land-use change, showing
18
19 93 that catchment information does not influence the general direction and magnitude of these
20
21 94 predictions. We discuss the implications of this work in Section 5, with a focus on the
22
23 95 importance of climate change relative to land-use change; we suggest that parsimonious
24
25 96 monthly models have practical utility when calibration data are available and when the main
26
27 97 objective of the study is to explore the *relative* effect of land use or climate change on seasonal
28
29 98 flow.
30
31
32
33
34
35
36
37

100 **2 A simple monthly water balance model for environmental change**

101 **2.1 Overview and comparison with other models**

102 The model used in this study, DWBM, is a four-parameter lumped catchment model that
103 partitions monthly precipitation into evapotranspiration and runoff (see full description in section
104 2.2). DWBM was developed by Zhang et al. (2008) with the aim to extend the Budyko theory, or
105 “limits” concept, to sub-annual timescales (Budyko, 1961; Hamel and Guswa, 2015). The model
106 also has a five-parameter version (Wang et al., 2011) but for the purpose of this study, we
107 employ the more parsimonious version, which has been verified on a subset of >200
108 catchments in Australia (Zhang et al. 2008).

1
2
3 109 DWBM is similar to a number of parsimonious lumped models, including *abcd* and G2M
4
5 110 (Mouelhi et al., 2006), which represent a catchment with one or two stores of water that
6
7 111 influence the basin-scale partitioning of precipitation into evapotranspiration and runoff. These
8
9 112 models continue to receive attention from the hydrologic community given the uncertainty
10
11 113 associated with complex models: for example, in their study of 429 catchments around the
12
13 114 world, Perrin et al. (2001) showed that models with a low number of parameters (<5) achieved a
14
15 115 performance comparable to more complex models, and recommended their use due to the ease
16
17 116 of assessing parameter uncertainty with such models. As described later, DWBM has the
18
19 117 advantage of using parameters with physical meaning, which facilitates interpretation of results
20
21 118 and inferring the effects of landscape modification. In general, we note that the selection of
22
23 119 DWBM does not impact the scope and ideas implemented in this study. Similar analyses could
24
25 120 be conducted with alternative models, and we suggest that a number of findings would hold: the
26
27 121 “equifinality of model structures”, as defined by Perrin et al. (2001), suggest that most
28
29 122 parsimonious models would yield similar results.
30
31
32
33

34 123 **2.2 Model description**

- 37 124 • Model equations

38
39
40 125 The DWBM model operates with two stores of water for a catchment – the vadose zone and
41
42 126 groundwater. Monthly precipitation is partitioned among direct runoff, evapotranspiration,
43
44 127 storage in the vadose zone, and recharge to groundwater; monthly streamflow is a combination
45
46 128 of direct runoff and baseflow supplied by the groundwater store. The following section describes
47
48 129 the main equations but the reader is referred to the full description of model development for
49
50 130 additional details (Zhang et al. 2008).
51
52
53

54 131 For each month, the model first partitions precipitation into catchment wetting and direct runoff.
55
56 132 Catchment wetting, X , for a month, m , is bounded by both a supply limit (P_m , the precipitation
57
58
59
60

1
2
3 133 arriving in that month) and a demand limit, X_0 . Mathematically, this “limit” concept is captured by
4
5 134 a bi-asymptotic function (Figure 1), and catchment wetting is computed as:
6
7

$$X(m) = P(m)F\left(\frac{X_0}{P(m)}, \alpha_1\right)$$

8
9
10
11
12
13 135 [1]
14

15
16 136 Where F is the bi-asymptotic function, defined as:
17

$$18$$

$$19 137 F(x, \alpha) = 1 + x - \left(1 + x^{\frac{1}{1-\alpha}}\right)^{1-\alpha},$$

$$20$$

$$21$$

$$22$$

23 138 [2]
24

25
26 139 α_1 is the retention efficiency, which determines how close X is to the supply and demand limits;
27

28 140 the “demand limit” X_0 is calculated as the sum of available storage capacity and
29

30 141 evapotranspiration demand, (here called potential evapotranspiration, PET):
31

$$32$$

$$33 X_0(m) = S_{max} - S(m - 1) + PET(m)$$

$$34$$

$$35$$

36 142 [3]
37

38
39 143 where S_{max} is the maximum catchment storage capacity and S the catchment storage value at a
40

41 144 given time step.
42

43
44 145 [FIGURE 1]
45

46
47 146
48
49

50
51 147 For each month, X is used to compute an intermediate variable, available water, W :
52

$$53$$

$$54 W(m) = X(m) + S(m - 1)$$

$$55$$

56
57 148 [4]
58

1
2
3 149 as well as the direct flow, Q_d , i.e. water not retained in the catchment that quickly becomes
4
5 150 streamflow:
6
7

$$Q_d(m) = P(m) - X(m)$$

8
9
10
11 151 [5]
12
13

14 152 The available water, W , is partitioned among evapotranspiration, storage and recharge. To do
15
16 153 so, the model computes the evapotranspiration opportunity, Y , i.e. the proportion of available
17
18 154 water that does not percolate below the root zone and become recharge. The supply limit for Y
19
20 155 is the available water, while the demand limit is the sum of potential evapotranspiration and
21
22 156 storage; therefore
23
24

$$Y(m) = W(m) \times F\left(\frac{PET(m) + S_{max}}{W(m)}, \alpha_2\right)$$

25
26
27
28
29
30 157 [6]
31
32

33 158 where α_2 is the evapotranspiration efficiency, which determines how close Y is to the supply and
34
35 159 demand limits (Figure 1).
36
37

38 160 Monthly evapotranspiration, ET , is bounded by the available water and energy demand (PET). It
39
40 161 is assumed that ET follows the same function as Y , i.e. that the evapotranspiration efficiency α_2
41
42 162 also determines how close ET is to the evapotranspiration demand:
43
44

$$ET(m) = W(m) \times F\left(\frac{PET(m)}{W(m)}, \alpha_2\right)$$

45
46
47
48
49
50 163 [7]
51
52

53 164 Recharge can then be calculated as the difference between available water and
54
55 165 evapotranspiration opportunity:
56
57
58
59
60

$$R(m) = W(m) - Y(m)$$

166 [8]

167 and storage is the difference between evapotranspiration opportunity and actual
 168 evapotranspiration:

$$S(m) = Y(m) - ET(m)$$

169 [9]

170 Finally, monthly baseflow is calculated as:

$$Q_b(m) = d \cdot G(m - 1)$$

171 [10]

172 where d is the groundwater store time constant, characterizing the groundwater drainage rate,
 173 and G is groundwater storage, updated monthly as:

$$G(m) = G(m - 1) - Q_b(m) + R(m)$$

174 [11]

175 Total streamflow is calculated as the sum of direct flow and baseflow.

176

- 177 • Interpretation in terms of environmental change

178 Given our focus on environmental change, we elaborate here on how climate and land-use
 179 changes can be represented by the model. Table 1 summarizes the expected relation between
 180 the four parameters and physical catchment characteristics. We suggest that changes in land-
 181 use and land-cover will likely affect S_{\max} , α_1 and α_2 : changes to root depth and soil properties

1
2
3 182 may alter the partitioning between direct runoff and soil storage, along with the partitioning of
4
5 183 soil water between groundwater recharge and evapotranspiration. The parameter d affects only
6
7 184 the monthly timing of baseflow, and we suggest that d is primarily a function of geology and not
8
9 185 significantly influenced by land use or climate changes. (At the daily time scale, the dynamic
10
11 186 storage theory suggests that it also depends on antecedent conditions, i.e., on land use and
12
13 187 climate features, cf. Kirchner, 2009).

16
17 188 Seasonal changes in precipitation and potential evapotranspiration will be captured by the
18
19 189 climate forcing variables. Changes in the intensity of individual precipitation events, a
20
21 190 characteristic not described by the monthly total, will likely affect α_1 , since higher intensity events
22
23 191 may result in more direct runoff. Indirect climate change effects may also affect soil and
24
25 192 vegetation properties, suggesting that α_2 and potentially S_{\max} may be affected by climate change
26
27 193 (Table 1).

28
29
30
31 194 [TABLE 1]

32
33
34 195
35
36
37
38
39
40
41
42
43
44
45
46
47
48
49
50
51
52
53
54
55
56
57
58
59
60

196 **3 Methods**

197 **3.1 Overview**

198 Our aim is to quantify the uncertainty in minimum flow predictions across a wide range of
199 climate and catchment characteristics, and to understand how this uncertainty evolves as
200 catchment information is introduced. Our analyses rely on two metrics, minimum monthly flow
201 (Q_{\min}) and total flow (Q_{tot}), computed as the minimum average monthly flow and average annual
202 flow, respectively, across the period of record. Here, minimum monthly flow is used to represent
203 dry-season flow, thereby using a flow-based definition of the dry season.

204 We first conduct a brief sensitivity analysis to illustrate the model response to climate forcing.
205 Building on previous work in Australia (Zhang et al. 2008), we compare observed minimum
206 monthly flows for 89 catchments to predictions from four versions of DWBM: one with
207 parameters obtained from calibration, two where parameters are determined via regression on
208 catchment characteristics, and one with no variation in model parameters among catchments
209 (i.e., the only variation in models among the basins is the climate forcing). We then use the
210 DWBM to predict low flows in 641 catchments in the United States. To assess the universality of
211 the regression models developed for the Australian catchments, we employ the same
212 regression models to determine model parameters for the US basins. We also evaluate the
213 performance of the DWBM with fixed parameters across the US catchments and with an
214 independent calibration. Finally, we explore the use of DWBM to assess the potential effect of
215 land-use change on dry-season flows for ungauged basins. In doing so, we evaluate whether
216 the model can predict land-use change effects in relative terms, even if the absolute magnitude
217 of minimum flows is not well predicted.

218

1
2
3 219 **3.2 Sensitivity analysis: relative importance of catchment characteristics on annual and**
4
5 220 **dry-season flow**
6
7

8 221 To demonstrate model behavior, we present the sensitivity of our two variables of interest,
9
10 222 minimum monthly flow and total flow, to both climate forcing and model parameters (which are
11
12 223 proxies for catchment characteristics). We present three distinct climates, subtropical-dry
13
14 224 summer, tropical-dry winter, and humid continental. Details of the analyses and in-depth
15
16 225 discussion of the hydrological processes driving the results are presented in Appendix 1.
17
18

19
20 226 **3.3 Parameter selection and model performance (Australian dataset)**
21

22 227 Given the physical interpretation of DWBM parameters (Section 2.2), we expect their values to
23
24 228 be correlated with measurable characteristics of a catchment. We tested this hypothesis on a
25
26 229 dataset of 89 catchments in Australia for which the DWBM model was calibrated using four
27
28 230 objective functions related to low flows, high flows, time shift, and total mass balance (Zhang et
29
30 231 al. 2008). Catchment areas vary between 50 and 2000 km² and are located across a large
31
32 232 range of climate zones (Figure 2a). We examined twelve relevant and readily available
33
34 233 catchment characteristics as explanatory variables for the regression, including information on
35
36 234 climate, soil, topography, and land use (Table 2). Data sources for catchment streamflow time
37
38 235 series and characteristics are described by Shao et al. (2012). Each catchment had at least 10
39
40 236 years of climate and streamflow data, which we used to run the model and obtain a time series
41
42 237 of monthly modeled streamflow. For both observed and modeled time series, we computed the
43
44 238 average monthly flows and extracted the minimum and total annual flow to obtain the values of
45
46 239 Q_{\min} and Q_{tot} for each catchment. After conducting a simple backward stepwise linear regression
47
48 240 model that had low predictive power (see Table 1), we developed two regression approaches
49
50 241 described below.
51
52
53
54
55

56 242
57
58
59
60

1
2
3 243 [FIGURE 2]
4
5

6 244 [TABLE 2]
7
8

9 245
10

- 11
12 246
- Regression with the full set of variables (regression trees)
- 13
14

15 247 We built regression trees to explore how much variability in parameter values could be

16
17 248 explained by the complete set of catchment characteristics given in Table 2. Regression trees

18
19 249 were selected for their high explanatory power, when compared with multiple linear regressions

20
21 250 and a multivariate adaptive regression spline (MARS) model (Shao et al., 2012). The analyses

22
23 251 were performed with the 'rpart'¹ package in the R environment. We tested simple and pruned

24
25 252 trees and finally selected a random forest method, using the 'randomForest'² package in R,

26
27 253 which gave the best performance. This method consists in creating thousands of unique

28
29 254 regression trees for the same dataset, using a random sampling of variables to create each tree

30
31 255 (Breiman, 2001). Each of these trees is used to predict the dependent variable, and the mean

32
33 256 prediction from the entire forest is the output. After "growing" a forest for each parameter, we

34
35 257 perform a 'leave-one-out' cross-validation, i.e. building a random forest using every observation

36
37 258 (the parameter values) except one, then using the model to predict the observation that was left

38
39 259 out. The process is repeated until the model has predicted every observation in the dataset,

40
41 260 after which the average prediction error is calculated.
42
43

- 44
45
46 261
- Multiple linear regression on a reduced set of variables
- 47
48

49 262 To assess the model performance in a situation with reduced data availability, we test a simple

50
51 263 linear regression model that relies on direct physical interpretation of parameters. Specifically,

52
53 264 we tested the correlation between each parameter and the catchment characteristics
54
55

56
57 ¹ <https://cran.r-project.org/web/packages/rpart/index.html>

58 ² <https://cran.r-project.org/web/packages/randomForest/index.html>
59
60

1
2
3 265 considered as the best proxies for the parameter. The following paragraphs explain the rationale
4
5 266 behind the selection of catchment characteristics for this simplified approach.
6
7

8
9 267 α_1 , the retention capacity, is closely related to the curve number (CN) used in the SCS-method
10
11 268 (NRCS-USDA, 2004). This empirical value captures the ability of a catchment to retain water in
12
13 269 the soil layer instead of producing direct runoff. Therefore, we tested the correlation between α_1
14
15 270 and CN values for each catchment. CN values were calculated as the weighted average of CN
16
17 271 for forest and grass land covers. Soil hydrologic groups were estimated from the HiHydroSoil
18
19 272 dataset (Boer, 2015)
20

21
22 273 α_2 is related to soil drainage and rain event frequency. Therefore, we used the subsoil hydraulic
23
24 274 conductivity and average storm depth as explanatory variables for α_2 .
25
26

27
28 275 S_{\max} is related to the product of soil depth and saturated water content. Because the soil dataset
29
30 276 we used did not show any variability in soil depths (all depths > 2400 mm), we only used
31
32 277 saturated water content in the regression.
33

34
35 278 d is related to hydraulic conductivity of deep layers. We used the subsoil hydraulic conductivity
36
37 279 as the only explanatory variable.
38

- 39
40 280
 - Mean parameters
41
42

43 281 We also tested a case for which no catchment-specific information is used to estimate the
44
45 282 parameters. For this, we used the mean values of the calibrated parameters across all
46
47 283 Australian catchments. For these analyses, only climate forcing varies among the models from
48
49 284 one catchment to the next.
50

- 51
52
53 285
 - Model performance
54
55
56
57
58
59
60

1
2
3 286 We ran the DWBM model three times for each Australian catchment with the parameter sets
4
5 287 described above, i.e. determined by the full regression model, the reduced regression model,
6
7 288 and the mean value. We compared the minimum flow and total flow predicted with each
8
9
10 289 parameterization, including the parameter set obtained by calibration, with the minimum flow
11
12 290 and total flow obtained from observed time series.

13 14 15 291 **3.4 Model verification (US dataset)**

16
17
18 292 We tested the performance of the modified DWBM, i.e. applied with the regressed set of
19
20 293 parameters, outside Australia. To compare the model performance when calibration data are
21
22 294 available, we also calibrated the model for the verification dataset. For this calibration, we used
23
24 295 a single objective function, the Nash-Sutcliffe efficiency for log-transformed flow, consistent with
25
26 296 our focus on low flows.

27
28
29 297 Our dataset of US catchments was developed by Newman et al. (2015), comprising 671
30
31 298 catchments (although we discarded 30 catchments for quality assurance reasons, see Appendix
32
33 299 B). Similar to the Australian dataset, the catchments range in size (1 to 25,800 km²) and
34
35 300 hydroclimatic conditions (Figure 2b). To run DWBM on the US dataset, we summed
36
37 301 precipitation data at the monthly time step and computed monthly potential evapotranspiration
38
39 302 from monthly temperature data, using the modified Hargreaves method (Eq. 5 from Droogers et
40
41 303 al., 2002). Q_{\min} and Q_{tot} and model performance metrics for the US dataset were calculated with
42
43 304 the method described above for the Australian dataset, i.e. we compared the Q_{\min} and Q_{tot}
44
45 305 predictions based on the three alternative parameterizations with observations. To further
46
47 306 explore the variability in model performance, we grouped results by region, according to the
48
49 307 USGS HUC 02 classification.
50
51
52
53
54
55
56
57
58
59
60

3.5 Variation of model performance with catchment characteristics

We examined the correlation between model errors and catchment characteristics to identify the conditions under which the model performs best. Specifically, we computed r^2 and p-values between errors in Q_{\min} and Q_{tot} obtained from each model parameterization, on one hand, and all catchment characteristics listed in Table 2, on the other hand.

3.6 Simulated effect of land-use change in ungauged basins

The parameters for the DWBM each incorporate the effects of a host of climate, landscape, and geologic factors, some of which are measurable and others which are not. Thus, detecting a land-use signal in the parameters when moving from one catchment to another may be challenging, as the effects of land-use alone may be lost amid the noise and other differences between the catchments. Nonetheless, we were interested in assessing model predictions of land-use change, in relative terms, within a particular catchment.

As noted in Table 1, land-use change presumably affects α_1 and α_2 . Over the longer term, land-use change may affect soil properties (i.e. S_{\max}), but this effect is arguably weaker and ignored in these analyses. It is possible that the flow response to a change in α_1 and α_2 , representing land-use change, may be a function of their original values. To test this hypothesis, we investigated the effect of simultaneous 10% and 20% changes in α_1 and α_2 for each Australian catchment, for both the calibrated dataset (for which the α_1 and α_2 parameters vary among the basins) and the mean-value dataset (which all share the same parameter values). If the changes in Q_{\min} that result from changes in α_1 and α_2 are comparable between the two models (calibrated and mean value), we can conclude that the effects of afforestation/deforestation on minimum flows are independent of the original parameter values. Thus, in an ungauged basin for which little information is available, the mean-value model could be used to predict the effects of land-use change. The values of relative change (10 and 20%) were based on the

1
2
3 332 maximum change in parameter values predicted by the random forest model: α_1 and α_2
4
5 333 increased by a maximum of 6% and 13%, respectively, when forest cover was increased by
6
7 334 66% (for catchments with a cover <34%).
8
9

10 335
11
12

14 336 **4 Results**

17 337 **4.1 Sensitivity analysis**

18
19 338 In general, the model shows greater sensitivity to parameters for the subtropical and tropical
20
21 339 climates (Figure 3). In the humid climate, catchment properties have a lower impact on
22
23 340 minimum flows, since evapotranspiration is primarily energy-limited and changes in catchment
24
25 341 water storage have little effect on hydrologic partitioning. In subtropical dry-summer and dry-
26
27 342 winter climates, a small decrease in α_1 or α_2 may lead to a sharp relative increase in Q_{\min} , due to
28
29 343 increases in the small amounts of surface runoff during dry months. Conversely, as α_1 or α_2
30
31 344 increase, Q_{\min} generally decreases as water retained in the soil store is more likely to be
32
33 345 evapotranspired.
34
35

36
37 346 Based on the above analyses, predictions of minimum flows will be minimally impacted by
38
39 347 changes in parameter values when: climate is humid with low seasonality in precipitation, i.e.
40
41 348 variability in evaporative demand is the main driver of minimum flows; and when catchment
42
43 349 properties correspond to “insensitive” ranges for model parameters. For example, Figure 3
44
45 350 shows that minimum flows are not sensitive to low values of α_1 for the tropical dry-winter
46
47 351 climate. In such climate, minimum flows in catchments with low retention capacity (e.g. with
48
49 352 clayey or compacted soils) are unlikely to be affected by land use change.
50
51

52 353
53
54

55
56 354 [FIGURE 3]
57
58
59
60

1
2
3 3554
5
6 3567
8 357 **4.2 Regression models for DWBM's parameters**9
10
11 358 The results from the random forest model are summarized in Table 3, showing that r^2 was high12
13 359 for all parameters. The mean predictive errors obtained with the random forest method for α_1 ,14
15 360 α_2 , S_{\max} , and d are reported in Table 3 and represent 45%, 39%, 40%, and 42% of their16
17 361 respective mean value (Table 3). To gauge the impact of errors of this magnitude on model18
19 362 outputs, we plotted these error ranges on the sensitivity analyses graphs (Figure 3): the effect of20
21 363 parameter errors was relatively low for Q_{tot} , but for the semi-arid and tropical climates, errors in22
23 364 α_2 and d may affect Q_{min} significantly (>50% error). In addition, the reduced regression model24
25 365 showed much less explanatory power (Table 3): the reduced set of variables explaining less26
27 366 than 20% of the variance in the calibrated parameter set.28
29
30
31 367 Of the thirteen variables in Table 2, the curve number CN ranked as the most important variable32
33 368 for α_1 and forest cover as the fourth most important variable. Here, importance is computed as34
35 369 follows (see details in footnote 2 above): the mean square error is calculated on the out-of-bag36
37 370 portion of the dataset, and again on the dataset with permuted variable; then, the average38
39 371 difference in mean square error over all trees is computed, and normalized by the standard40
41 372 deviation of the differences. For α_2 , the four most important variables were all climate-related42
43 373 (Peomonths, Aridity, Precipitation,CVP).44
45
46
47 37448
49
50 375 [TABLE 3]51
52
53 376
54
55
56
57
58
59
60

377 4.3 Model performance (Australian dataset)

378 Figure 4 and Table 4 illustrate the model performance for Q_{\min} for the Australian dataset.

379 Comparison of results from the calibrated models to the observed minimum flows yielded a root-
380 mean-square error (RMSE) of 2.37 mm/mo (i.e. about 50% of the average minimum flow, 4.63
381 mm/mo). The model with parameters obtained from the full regression ("full regression model"
382 hereafter) yielded good results for Q_{\min} , with a RMSE of 2.32 mm/mo (Table 4) – similar to the
383 performance of the calibrated models. Model performance was lower when using the reduced
384 regression or the mean values for parameters, although these models still explained a large
385 proportion of the variance in Q_{\min} (>53%).

386 The four models predicted total flows well, with r^2 values >0.87 (Table 4). The lowest RMSE for
387 total flows was obtained by the model with calibrated values (RMSE=42.4 mm/year), and the
388 highest was obtained by the model with mean values.

390 [FIGURE 4]

391 [TABLE 4]

392

393 4.4 Model verification (US dataset)

394 With the parameters obtained from the full regression, the performance of DWBM for minimum
395 flows was lower in the US (Table 4). The model explained 92% of the variance in Q_{tot} , but only
396 between 51 and 55% of the variance in Q_{\min} (Table 4, Figure 5). As information was introduced
397 by the full regression and reduced regression, there was no improvement in model performance
398 over the mean-value model (RMSE in Q_{\min} for the simplified regression was lower than the full
399 regression but the difference was not statistically significant, based on a Kolmogorov-Smirnov

1
2
3 400 test). However, calibration of the models based on log-transformed Nash-Sutcliffe efficiency
4
5 401 resulted in much higher performance –with 88% of the variance in Q_{\min} explained, similar to the
6
7 402 Australian dataset. The calibrated value ranges were slightly broader than those of the
8
9
10 403 Australian dataset, [0.36;0.99], [0.16; 0.94], [0.10; 1], and [32; 500], respectively, for α_1 , α_2 ,
11
12 404 S_{\max} , and d (Australian ranges are reported in Table 3).
13
14
15 405
16
17
18 406 [FIGURE 5]
19
20
21 407
22
23

24 408 **4.5 Correlation between errors in Q_{\min} and catchment characteristics**

25
26 409 When using the calibrated parameters for the Australian catchments, we found significant
27
28 410 correlations ($p < 0.01$) between the relative error in minimum flow and three catchment
29
30 411 characteristics: aridity, precipitation, and PAWHC (all negative correlations). Errors in total flow
31
32 412 also showed strong correlations with catchment characteristics, in particular with climate
33
34 413 variables, and soil properties.
35
36
37

38 414 When using model predictions from the full regression model, errors in minimum flow showed
39
40 415 significant correlation only with the aridity index, and errors in total flow with precipitation and
41
42 416 the aridity index. No correlation was found for any catchment characteristics for predictions
43
44 417 obtained with the reduced regression or mean models.
45
46
47

48 418 We found no significant correlation between catchment characteristics and relative errors in
49
50 419 minimum flows for the US catchments, for any parameter set. However, relative errors in total
51
52 420 flows were correlated with a number of catchment characteristics (all variables in Table 2 except
53
54 421 CN and the relief ratio), and with two parameters (positive correlation, for both α_2 , and d).
55
56
57
58
59
60

1
2
3 422 To explore the regional variation in model performance in the US, we separated the catchments
4
5 423 by region, using the USGS HUC 2 classification (Figure 2). Across these more homogenous
6
7 424 units, the calibrated model performance varied without significant pattern. However, the
8
9 425 improvement upon regression and mean-value models is more appreciable for HUCs with
10
11 426 higher values, which comprise more arid regions, a finding that seems consistent with the higher
12
13 427 performance of the model in arid catchments in Australia.
14
15
16
17 428

20 429 **4.6 Simulated effect of land-use change in ungauged basins**

21
22
23 430 Figure 6a represents the relative change in Q_{\min} following 10% and 20% changes (both positive
24
25 431 and negative) in α_1 and α_2 . All values in the bottom-left quadrant represent an increase in α_1 and
26
27 432 α_2 , while all values in the top-right quadrant represent a decrease in the two parameters. The
28
29 433 direction of the change is consistent between the calibrated and mean datasets. The difference
30
31 434 in Q_{\min} predicted by the models was small for the 10% change in parameter (RMSE of 0.36). For
32
33 435 the 20% change, the high RMSE (1.2) was largely driven by the negative change in parameter
34
35 436 values (i.e. circles in the top-right quadrant in Figure 6a). Of note, these high relative changes
36
37 437 correspond to low absolute changes: the RMSE for the absolute change in Q_{\min} resulting from a
38
39 438 20% change (both positive and negative) in parameters is 1.5mm.
40
41
42

43 439 The results for total flow (Figure 6b) showed even smaller differences between the two models,
44
45 440 indicating that medium to high flows were less affected, in relative terms, by the change in
46
47 441 parameter values. RMSE were 0.15 and 0.37, respectively, for the 10% and 20% change in
48
49 442 parameter values.
50

51
52
53 443

54
55
56 444 [FIGURE 6]
57
58
59
60

1
2
3 445

4
5
6
7 446 **5 Discussion and implications for predicting the effects of environmental**
8
9 447 **change**

10
11 448 The main objective of this paper is to assess the utility of a monthly, lumped hydrologic model
12
13 449 for predicting dry-season flows with varying degrees of information availability. As a rainfall-
14
15 450 runoff model governed by four parameters with physical meaning, DWBM has the potential to
16
17 451 be used for climate and land-use change scenarios analyses and inform landscape
18
19 452 management. The sensitivity analyses indicated that the importance of each parameter
20
21 453 depends on climate: for example, a larger storage capacity S_{\max} will generally be needed in
22
23 454 highly seasonal climate to sustain baseflow during the dry season. The moderate sensitivity in a
24
25 455 number of environmental contexts (i.e. parameter sets) suggests that climate is the main driver
26
27 456 of seasonal flow, a fact that has been observed by many others (Devito et al., 2005; Jencso and
28
29 457 McGlynn, 2011). In practice, this means that a rough estimate of these parameters may be
30
31 458 sufficient to predict monthly flows with acceptable levels of certainty, as suggested by our
32
33 459 analyses on Australian and US catchments.

34
35
36
37
38 460 **5.1 Model performance for absolute predictions of dry-season flow**

39
40
41 461 The model performance, measured by r^2 , in Australia was relatively high for both Q_{\min} and Q_{tot}
42
43 462 predictions (Figure 4). RMSE for Q_{\min} ranged from 2.4 mm/mo to 4.0 mm/mo, depending on the
44
45 463 model parameterization. Adding catchment information, i.e. moving from uniform parameters for
46
47 464 all catchments, to regressed parameter values, to streamflow time series for calibration,
48
49 465 generally improved model performance (measured by RMSE). The performance of the full
50
51 466 regression model was actually as good as the calibrated model, probably due to the large
52
53 467 number of explanatory variables and the high explanatory power of the regression (Table 3).
54
55 468 The poorer performance of the reduced regression could be due to two factors: poor selection of
56
57
58
59
60

1
2
3 469 model variables and over-fitting of the random forest full regression model. The stepwise
4
5 470 backward regression conducted in preliminary analyses confirmed that our selected variables
6
7 471 are among the best predictors, but that no single variable explained the variance significantly.
8
9 472 This suggests that the full regression model was probably over-fitted (12 variables for 89
10
11 473 observations), and therefore less likely to transfer outside the initial sample, for the US
12
13 474 catchments.
14
15
16

17 475 For the verification dataset with US catchments, the performance of DWBM with parameters
18
19 476 derived from the full regression was much lower: only 55% of the variance in Q_{\min} was
20
21 477 explained. This suggests that although model parameters were strongly correlated with physical
22
23 478 characteristics in Australia, these relationships did not transfer to the US dataset. A number of
24
25 479 reasons could explain this negative result, in particular the consideration of snowmelt (see
26
27 480 below), and extrapolations of the regression outside the range of Australian values for a number
28
29 481 of physical characteristics (in particular soil variables and, to a lesser extent, climate variables).
30
31 482 However, after calibration, DWBM's performance was good for both total and minimum flows,
32
33 483 confirming the possibility to use the model with regional parameterization.
34
35
36

37 484 Because errors in Q_{\min} were only weakly correlated with catchment characteristics, it is difficult
38
39 485 to predict where the model will perform best outside the set of catchments in Australia or the
40
41 486 US. However, the model seemed to perform better when the aridity index was lower (i.e. drier,
42
43 487 and thus minimum flows were lower), likely reflecting water-balance constraints in a water-
44
45 488 limited environment. Additionally, it is likely that snowmelt effects, ignored in this work,
46
47 489 contribute to errors in minimum flows. To test this hypothesis, we evaluated model performance
48
49 490 for the 97 US basins that were not influenced by snow precipitation (Guswa et al., 2017), and
50
51 491 found that r^2 increased to 0.70 (from 0.55) and 0.68 (from 0.51), respectively, for the "full
52
53 492 regression" and mean-value parameterizations (RMSE were 4.4 mm and 4.5 mm, respectively).
54
55 493 These results confirm that the relationships did not transfer to the US dataset. We also
56
57
58
59
60

1
2
3 494 hypothesized that performance would be higher where high values of α_1 and α_2 are predicted by
4
5 495 the regression, based on the sensitivity analyses, although the US dataset did not confirm this
6
7 496 hypothesis.
8
9

10
11 497 We conclude this section with methodological points that help interpret model performance, both
12
13 498 for absolute values or theoretical land-use change. First, we note that many catchments in our
14
15 499 datasets had low observed minimum flow (<3mm/mo), especially for the Australian dataset
16
17 500 dominated by the “humid temperate warm summer” climate zone. In absolute values, these
18
19 501 errors remain small as illustrated by Figure 4. In addition, the datasets included only “natural”
20
21 502 catchments, with the land use being mainly grassland or forest. This means that the effect of
22
23 503 different land uses is likely difficult to detect in these datasets, as suggested by the regressions
24
25 504 on catchment characteristics (forest cover was not significantly correlated with α_1 or α_2). This
26
27 505 could also explain the poor performance of the reduced regression model: variations in α_1 and
28
29 506 α_2 based on the simple regression models were small (for example, CN values only varied from
30
31 507 70 to 80, a narrower range compared to possible land use changes involving agricultural land).
32
33
34

35 508 We also note that further analyses could improve model performance in both regions. First, the
36
37 509 model calibration could be focused on low flows. The calibration for the Australian dataset was
38
39 510 performed using a combination of four objective functions, with only one focused on low flows
40
41 511 (Zhang et al., 2008). Second, the parameter values could be corrected for the bias in Q_{\min} for
42
43 512 the US dataset. This bias may be related to the calibration function, but our analyses do not
44
45 513 provide evidence of this.
46
47
48

49 514 **5.2 Predicting the effect of environmental change for ungauged catchments**

- 50
51
52 515 • Climate change

53
54
55 516 Both the US and Australian dataset comprise catchments that range in climate, geology, and
56
57 517 land use. The fair performance of the model in both locations suggests that the model is able to
58
59
60

1
2
3 518 represent the variability of hydrological behavior induced by these factors. This gives confidence
4
5 519 that the effect of future climate forcing would be correctly represented: because the model uses
6
7 520 monthly climate time series as forcing variables, such analysis can be performed by substituting
8
9
10 521 current climate time series with future forecasts. Given the highest performance of the calibrated
11
12 522 model, climate change analyses are best performed with gauged catchments (calibrating the
13
14 523 model). However, they may be conducted on ungauged catchments too when information on a
15
16 524 relative change, rather than absolute, is sought. For example, Monte-Carlo-type analysis can be
17
18 525 performed by assuming parameter sets for the catchment of interest, and then running the
19
20 526 model for each set to provide upper and lower bounds of the expected change following climate
21
22
23 527 change.

- 24
25
26 528 • Land use change

27
28
29 529 The high performance of the full regression model in Australia was not found in the US.
30
31 530 Therefore, using model regression to infer parameter values is not a feasible option for
32
33 531 ungauged catchments globally. For the Australian dataset, CN and forest cover were found to
34
35 532 be important variables in the full regression on α_1 (Section 4.2), confirming the relationship
36
37 533 between this parameter and land-use variables. For both regions, calibrated parameter values
38
39 534 showed low or no correlation with land-use variables, which suggest that additional work is
40
41
42 535 needed to derive empirical relationships between the parameter values and land use
43
44 536 characteristics. Nonetheless, the land-use change analyses in Section 4.6 suggest that one can
45
46 537 use the baseline provided by the model to compute the relative change in Q_{\min} following land-
47
48 538 use change. The motivation for this simple analysis was to understand, theoretically, the effect
49
50 539 of landscape interventions on dry-season flows. For example, such information can be used to
51
52
53 540 assess the potential for the “sponge effect” to occur in a given climate (i.e. that afforestation
54
55 541 would increase dry-season flow): specifically, the catchments with a relative change close to
56
57
58
59
60

1
2
3 542 zero in Figure 6a are unlikely to demonstrate an increase in dry-season flow with afforestation,
4
5 543 since the change in α parameter values only minimally affected Q_{\min} .
6
7

8 544 We note that the absolute change in parameter values can be constrained by the calibrated
9
10 545 parameter set, if regional data are available (e.g. the US and Australian datasets used in this
11
12 546 study). As suggested above, Monte-Carlo runs can be performed to provide confidence intervals
13
14 547 around the change in Q_{\min} . Additional work on the relationships between catchment
15
16 548 characteristics and parameter is in progress with catchments that have pre- and post-
17
18 549 afforestation streamflow data (Zhang et al., 2016). Preliminary results suggest that the
19
20 550 relationships hypothesized in Table 1 hold and that regional relationships can be used to predict
21
22 551 land-use change. The results also confirm that the land-use change signal (i.e. the increase in
23
24 552 forest cover, with all other variables held constant) may be confounded by other environmental
25
26 553 factors.
27
28
29
30
31 554

32 33 34 555 **6 Conclusion**

35
36
37 556 We have investigated how a simple rainfall-runoff model run at the monthly time step could
38
39 557 represent and predict the influence of climate and land-use change on dry-season flow. We
40
41 558 used the DWBM model, which assumes that streamflow, in particular during the dry season, is
42
43 559 driven by four main catchment characteristics: the retention efficiency of a catchment (ability to
44
45 560 store water for future release by discharge or evapotranspiration), evapotranspiration efficiency
46
47 561 (ability to use soil water for evapotranspiration rather than discharge), total soil storage, and
48
49 562 drainage rate. Our analyses confirmed that climate is a major driver of seasonal flows and that
50
51 563 the simple model DWBM, with default values obtained from the mean of calibrated catchments,
52
53 564 could provide a reasonable estimate of monthly flows. Model performance increases
54
55 565 significantly when calibration data are available, although in this work we found that regional
56
57
58
59
60

1
2
3 566 relationships to infer model parameters could not transfer to other regions (the regression on
4
5 567 catchment properties obtained in Australian did not result in high performance in the US). Our
6
7 568 analyses also suggest that DWBM can be used to estimate a change in annual and minimum
8
9 569 monthly flow following environmental change. Even without calibration data, the effects of land
10
11 570 use change (e.g. reduction in retention efficiency or in evapotranspiration efficiency) can be
12
13 571 explored and quantitatively estimated. The effect of climate change can also be assessed,
14
15 572 preferably with a calibrated model if absolute values are sought. The broad range of
16
17 573 environmental conditions used in that study confirmed that the simple structure is able to
18
19 574 capture the main hydrological processes driving runoff response. The model has low data
20
21 575 requirements, and all climate data and catchment information used in this study are available
22
23 576 globally.
24
25
26
27
28 577

31 578 **Acknowledgements**

32
33
34 579 The authors are grateful for the support from The Natural Capital Project, with funding from
35
36 580 Google.org (grant #172761).
37
38
39 581

42 582 **References**

43
44
45 583 Andréassian, V., 2004. Waters and forests: From historical controversy to scientific debate. J.
46
47 584 Hydrol. 291, 1–27. doi:10.1016/j.jhydrol.2003.12.015
48
49
50 585 Boer, F. de, 2015. HiHydroSoil: A High Resolution Soil Map of Hydraulic Properties. Report 134;
51
52 586 www.futurewater.nl.
53
54
55 587 Brauman, K.A., Richter, B.D., Postel, S., Malsy, M., Flörke, M., 2016. Water depletion: An
56
57
58
59
60

- 1
2
3 588 improved metric for incorporating seasonal and dry-year water scarcity into water risk
4
5 589 assessments. *Elem. Sci. Anthr.* 4, 83. doi:10.12952/journal.elementa.000083
6
7
8
9 590 Breiman, L., 2001. Random Forests, in: *Machine Learning*. pp. 5–32.
10
11 591 doi:10.1023/A:1010933404324
12
13
14 592 Brown, A.E., Western, A.W., McMahon, T.A., Zhang, L., 2013. Impact of forest cover changes
15
16 593 on annual streamflow and flow duration curves. *J. Hydrol.* 483, 39–50.
17
18 594 doi:10.1016/j.jhydrol.2012.12.031
19
20
21 595 Brown, A.E., Zhang, L., McMahon, T. a., Western, A.W., Vertessy, R. a., 2005. A review of
22
23 596 paired catchment studies for determining changes in water yield resulting from alterations
24
25 597 in vegetation. *J. Hydrol.* 310, 28–61. doi:10.1016/j.jhydrol.2004.12.010
26
27
28 598 Brutsaert, W., 2008. Long-term groundwater storage trends estimated from streamflow records:
29
30 599 Climatic perspective. *Water Resour. Res.* 44, n/a-n/a. doi:10.1029/2007WR006518
31
32
33
34 600 Budyko, M., 1961. *The Heat Balance of the Earth's Surface*. Washington D.C.
35
36
37 601 Devito, K., Creed, I., Gan, T., Mendoza, C., Petrone, R., Silins, U., Smerdon, B., 2005. A
38
39 602 framework for broad-scale classification of hydrologic response units on the Boreal Plain :
40
41 603 is topography the last thing to consider ? *Hydrol. Process.* 19, 1705–1714.
42
43 604 doi:10.1002/hyp.5881
44
45
46 605 Gao, Z., Zhang, L., Cheng, L., Zhang, X., Cowan, T., Cai, W., Brutsaert, W., 2015. Groundwater
47
48 606 storage trends in the Loess Plateau of China estimated from streamflow records. *J. Hydrol.*
49
50 607 530, 281–290. doi:10.1016/j.jhydrol.2015.09.063
51
52
53
54 608 Gehne, M., Hamill, T., Kiladis, G.N., Trenberth, K.E., 2016. Comparison of Global Precipitation
55
56 609 Estimates across a Range of Temporal and Spatial Scales. *J. Clim.*
57
58
59
60

- 1
2
3 610 Guswa, A., Brauman, K.A., Brown, C., Hamel, P., Keeler, B.L., Sayre, S.S., 2014. Ecosystem
4
5 611 Services: Challenges and Opportunities for Hydrologic Modeling to Support Decision
6
7 612 Making. *Water Resour. Res.* 50, 4535–4544. doi:10.1002/2014WR015497
8
9
10 613 Guswa, A.J., Hamel, P., Dennedy-Frank, P.J., 2017. Potential effects of landscape change on
11
12 614 water supplies in the presence of reservoir storage. *Water Resour. Res.*
13
14
15 615 Hamel, P., Guswa, A.J., 2015. Uncertainty analysis of a spatially-explicit annual water-balance
16
17 616 model: case study of the Cape Fear catchment, NC. *Hydrol. Earth Syst. Sci.* 19, 839–853.
18
19 617 doi:10.5194/hess-19-839-2015
20
21
22 618 Hughes, D.A., 2004. Incorporating groundwater recharge and discharge functions into an
23
24 619 existing monthly rainfall–runoff model/Incorporation de fonctions de recharge et de vidange
25
26 620 superficielle de nappes au sein d’un modèle pluie-débit mensuel existant. *Hydrol. Sci. J.*
27
28 621 49. doi:10.1623/hysj.49.2.297.34834
29
30
31
32 622 Jencso, K.G., McGlynn, B.L., 2011. Hierarchical controls on runoff generation: Topographically
33
34 623 driven hydrologic connectivity, geology, and vegetation. *Water Resour. Res.* 47, n/a-n/a.
35
36 624 doi:10.1029/2011WR010666
37
38
39 625 Kirby, J.M., Connor, J., Ahmad, M.D., Gao, L., Mainuddin, M., 2014. Climate change and
40
41 626 environmental water reallocation in the Murray–Darling Basin: Impacts on flows, diversions
42
43 627 and economic returns to irrigation. *J. Hydrol.* 518, 120–129.
44
45 628 doi:10.1016/j.jhydrol.2014.01.024
46
47
48
49 629 Kirchner, J.W., 2009. Catchments as simple dynamical systems: Catchment characterization,
50
51 630 rainfall-runoff modeling, and doing hydrology backward. *Water Resour. Res.* 45, W02429.
52
53
54 631 McIntyre, N., Ballard, C., Bruen, M., Bulygina, N., Buytaert, W., Cluckie, I., Dunn, S., Ehret, U.,
55
56 632 Ewen, J., Gelfan, A., Hess, T., Hughes, D., Jackson, B., Kjeldsen, T., Merz, R., Park, J.,
57
58
59
60

- 1
2
3 633 Connell, E.O., Donnell, G.O., Oudin, L., Todini, E., Wagener, T., Wheeler, H., McIntyre, N.,
4
5 634 2014. Modelling the hydrological impacts of rural land use change. *Hydrol. Res.* 45, 737–
6
7 635 754. doi:10.2166/nh.2013.145
8
9
10 636 Mouelhi, S., Michel, C., Perrin, C., Andréassian, V., 2006. Stepwise development of a two-
11
12 637 parameter monthly water balance model. *J. Hydrol.* 318, 200–214.
13
14 638 doi:10.1016/j.jhydrol.2005.06.014
15
16
17
18 639 Newman, A.J., Clark, M.P., Sampson, K., Wood, A., Hay, L.E., Bock, A., Viger, R.J., Blodgett,
19
20 640 D., Brekke, L., Arnold, J.R., Hopson, T., Duan, Q., 2015. Development of a large-sample
21
22 641 watershed-scale hydrometeorological data set for the contiguous USA: data set
23
24 642 characteristics and assessment of regional variability in hydrologic model performance.
25
26 643 *Hydrol. Earth Syst. Sci.* 19, 209–223. doi:10.5194/hess-19-209-2015
27
28
29
30 644 NRCS-USDA, 2004. Chapter 10. Estimation of Direct Runoff from Storm Rainfall, in: United
31
32 645 States Department of Agriculture (Ed.), Part 630 Hydrology. National Engineering
33
34 646 Handbook. United States Department of Agriculture,
35
36 647 <http://www.nrcs.usda.gov/wps/portal/nrcs/detailfull/national/water/?cid=stelprdb1043063>.
37
38
39 648 Perrin, C., Michel, C., Andréassian, V., 2001. Does a large number of parameters enhance
40
41 649 model performance? Comparative assessment of common catchment model structures on
42
43 650 429 catchments. *J. Hydrol.* 242, 275–301. doi:http://doi.org/10.1016/S0022-
44
45 651 1694(00)00393-0
46
47
48
49 652 Price, K., 2011. Effects of watershed topography, soils, land use, and climate on baseflow
50
51 653 hydrology in humid regions: A review. *Prog. Phys. Geogr.* 35, 465–492. doi:DOI:
52
53 654 10.1177/0309133311402714
54
55
56 655 Shao, Q., Traylen, A., Zhang, L., 2012. Nonparametric method for estimating the effects of
57
58
59
60

- 1
2
3 656 climatic and catchment characteristics on mean annual evapotranspiration. *Water Resour.*
4
5 657 *Res.* 48, 1–13. doi:10.1029/2010WR009610
6
7
8 658 Smakhtin, V., Hughes, D., 2007. Automated estimation and analyses of meteorological drought
9
10 659 characteristics from monthly rainfall data. *Environ. Model. Softw.* 22, 880–890.
11
12 660 doi:10.1016/j.envsoft.2006.05.013
13
14
15
16 661 Smith, M.B., Seo, D.-J., Koren, V.I., Reed, S.M., Zhang, Z., Duan, Q., Moreda, F., Cong, S.,
17
18 662 2004. The distributed model intercomparison project (DMIP): motivation and experiment
19
20 663 design. *J. Hydrol.* 298, 4–26. doi:10.1016/j.jhydrol.2004.03.040
21
22
23 664 Vogl, A.L., Denny-Frank, P.J., Wolny, S., Johnson, J.A., Hamel, P., Narain, U., Vaidya, A.,
24
25 665 2016. Managing forest ecosystem services for hydropower production. *Environ. Sci. Policy*
26
27 666 61, 221–229.
28
29
30 667 Wang, Q.J., Pagano, T.C., Zhou, S.L., Hapuarachchi, H. a P., Zhang, L., Robertson, D.E., 2011.
31
32 668 Monthly versus daily water balance models in simulating monthly runoff. *J. Hydrol.* 404,
33
34 669 166–175. doi:10.1016/j.jhydrol.2011.04.027
35
36
37
38 670 Zhang, L., Brutsaert, W., Crosbie, R., Potter, N., 2014. Long-term annual groundwater storage
39
40 671 trends in Australian catchments. *Adv. Water Resour.* 74, 156–165.
41
42 672 doi:10.1016/j.advwatres.2014.09.001
43
44
45 673 Zhang, L., Hickel, K., Shao, Q., 2016. Predicting afforestation impacts on monthly streamflow
46
47 674 using the DWBM model. *Ecohydrology* 10. doi:10.1002/eco.1821
48
49
50 675 Zhang, L., Potter, N., Hickel, K., Zhang, Y., Shao, Q., 2008. Water balance modeling over
51
52 676 variable time scales based on the Budyko framework – Model development and testing. *J.*
53
54 677 *Hydrol.* 360, 117–131. doi:10.1016/j.jhydrol.2008.07.021
55
56
57
58
59
60

1
2
3 678
4
5
6 679
7
8
9
10 680
11
12
13
14
15
16
17
18
19
20
21
22
23
24
25
26
27
28
29
30
31
32
33
34
35
36
37
38
39
40
41
42
43
44
45
46
47
48
49
50
51
52
53
54
55
56
57
58
59
60

For Peer Review

681 Appendix

682 A. Sensitivity analysis

683 We performed the sensitivity analyses with actual data from three climatically distinct locations:
684 (1) Nairobi, Kenya, (2) San Jose, Costa Rica, and (3) Cleveland, USA. Under the Köppen-
685 Geiger climate classification, Nairobi has a subtropical highland climate with dry summers and
686 an annual aridity index of 0.47; San Jose has a tropical climate, with dry winter and an aridity
687 index of 1.6; Cleveland has a humid continental climate with an aridity index of 2.4. Although we
688 could have used synthetic climate series to control climate variability, our objective here is to
689 illustrate model behaviors under different climate forcing, which is achieved by actual data from
690 different climate zones.

- 691 • Methods

692 Monthly precipitation and temperature data were acquired for each of these locations from the
693 National Oceanic and Atmospheric Administration's (NOAA) Global Historical Climatology
694 Network-Monthly (GHCN-M) dataset. From this dataset, we computed monthly averages. The
695 precipitation averages were used directly as model input, while the temperature averages were
696 used to calculate monthly potential evapotranspiration (PET) values using the modified
697 Hargreaves method (equation (5) from Droogers, et al., 2002). The precipitation and potential
698 evapotranspiration time series for each location are shown in Figure A1.

699 For each climate type, we first performed a one-at-a-time sensitivity analysis, using five levels at
700 equal intervals for each parameter. The range for each parameter was initially based on the
701 values obtained from the model calibration by Zhang et al. (2008), described in further details in
702 Section 3, and summarized in Table A1. Initial conditions affected flows for only the first few

1
2
3 703 years: to remove this 'warm-up' effect, the model was run for 10 years, repeating the same
4
5 704 climate forcing, and only the final year was used to compute the statistics.
6
7

8 705 Next, to quantify interaction effects among parameters, the model was run 24 additional times
9
10 706 for each climate type, varying every possible pair of parameters with all possible combinations
11
12 707 of upper and lower bounds for each parameter.
13
14

15
16 708 After computing the regression analyses (cf. Section 3.1), we also re-ran the one-at-a-time
17
18 709 sensitivity analyses varying mean values of each parameter by the average error in the random
19
20 710 forest model: the new range (twice the average parameter error around the mean value) gives a
21
22 711 more realistic assessment of sensitivity for the Australian dataset, and is plotted on Figure 3.
23
24

25 712 [TABLE A1 and FIGURE A1]
26
27

28 713 • Results
29
30

31 714 In general, for the humid continental climate (Cleveland), total flow and minimum flow (Q_{\min})
32
33 715 were not very sensitive to model parameters (Figure 3). The highest change in Q_{\min} was 42%,
34
35 716 obtained for the minimum value of α_2 . We note that in absolute value, effects of parameter
36
37 717 change were more significant than for other climates: for example, the 42% change in Q_{\min}
38
39 718 represented 23 mm/mo. Larger variations in the relative sensitivity were observed for the two
40
41 719 other climate types.
42
43
44

45 720 α_1 In the tropical dry winter (San Jose) and subtropical dry summer (Nairobi) climates, Q_{\min} was
46
47 721 sensitive to increases in α_1 (with a maximum change of 53%) due to less direct flow during and
48
49 722 slightly after each precipitation event. In Nairobi, Q_{\min} was more sensitive to low values of α_1 :
50
51 723 decreasing α_1 lowers the baseflow contribution to streamflow significantly by reducing the
52
53 724 amount of water that is retained in soil storage, and thus in groundwater storage.
54
55
56
57
58
59
60

1
2
3 725 α_2 . In the tropical and subtropical climates, Q_{\min} decreased as α_2 increased (-83% and -96%,
4
5 726 respectively), due to a larger portion of water being evapotranspired. Q_{\min} was sensitive to lower
6
7 727 values of α_2 in Nairobi (subtropical dry-summer), since evapotranspiration demand is high when
8
9 728 flows are low.

11
12
13 729 S_{\max} . In all three climates, Q_{\min} showed little sensitivity to S_{\max} . Lower values tended to increase
14
15 730 Q_{\min} in Nairobi, since they increased evapotranspiration opportunity (i.e. evapotranspiration and
16
17 731 recharge) in an arid environment. Conversely, lower values tended to decrease Q_{\min} in San
18
19 732 Jose (tropical dry-winter) where water availability is higher, and low soil storage increased the
20
21 733 ratio of direct runoff over recharge.

22
23
24 734 d. As expected, Q_{\min} was highly sensitive to d in seasonal climates (subtropical and tropical). In
25
26 735 particular, lower values of d resulted in sharp increases in Q_{\min} , since the slow groundwater
27
28 736 release sustained a high baseflow throughout the year.
29
30
31
32 737 Interaction effects showed mostly subadditive effects. Only low values of d tended to exacerbate
33
34 738 sensitivity to S_{\max} or α_2 , while low values of S_{\max} tended to exacerbate sensitivity to α_1 or α_2 .

35
36
37 739

40 740 **B. Quality assurance of Newman's dataset (2015)**

41
42
43 741 [TABLE B1]
44
45
46
47
48
49
50
51
52
53
54
55
56
57
58
59
60

742 TABLES

743 *Table 1. Parameters and physical interpretation of DWBM. + and ++ indicate the strength of the likely*
 744 *effect of land use change (LUC) and climate change (CC) on the parameters. Numbers in brackets are*
 745 *coefficients obtained from a stepwise backward linear regression between calibrated parameter values*
 746 *and forest cover (for LUC), or number of wet days (for CC) (* indicates significance at the 0.1 level, ***
 747 *significance at the 0.01 level). See text and Table 2 for a definition of these variables.*

Parameter	Description	Affected by	Affected by
		LUC	CC
S_{\max}	Maximum catchment storage capacity.	+	+
[5; 500]mm	<i>Depends on:</i> soil depth and available water content (measurable soil characteristics)	[0.71]*	[-309]*
α_1 [0;1]	Catchment retention; affects the partitioning of precipitation into direct runoff and water that is available in the soil-moisture store (S) for evapotranspiration and groundwater recharge. <i>Depends on:</i> the soil infiltration capacity and the rainfall intensity (more intense, less frequent events means more direct runoff).	++ [1.8e ⁻⁴]	++ [-0.15]
α_2 [0;1]	Evapotranspiration efficiency; affects the partitioning of soil water into storage, recharge, and actual evapotranspiration. <i>Depends on:</i> the rainfall frequency, plant water-stress response, root depth, and soil properties such as hydraulic conductivity and critical moisture content (at which actual evapotranspiration is reduced for water	++ [4.1e ⁻⁴]	+ [-0.30]**

stress). Note that α_2 does not depend on the crop coefficient, which is already included in PET

d [0;1] month⁻¹	Groundwater store time constant; characterizes the groundwater drainage rate, ie the release of groundwater storage to baseflow. Note that d does not affect partitioning, only timing of baseflow. <i>Depends on:</i> aquifer characteristics (size, hydraulic conductivity, connectivity with the stream)	n.a.	n.a.
-----------------------------------	--	------	------

748

749 *Table 2. Catchment characteristics assessed in this study*

	Abbreviation	Name	Description
Climate	P	Precipitation (mm/month)	Monthly rainfall
	Aridity	Aridity (-)	Precipitation divided by Potential Evapotranspiration
	Peomonths	Difference in peak potential evapotranspiration and precipitation (month)	The number of months that peak precipitation follows peak potential evapotranspiration
	ASD	Average Storm Depth (mm/day)	Depth of the average storm
	WetDays	Proportion of Wet Days (-)	Proportion of days per year with some precipitation
	CVP	Coefficient of Variation of Precipitation (-)	The standard deviation (of interannual precipitation) divided by the average

			annual rainfall
Vegetation	forest	Forest Cover (%)	Percent of catchment area covered by forest
	CN	Curve Number	Curve Number from the SCS method (also a function of soil group)
Topography	Rr	Relief Ratio (m/m)	Total catchment relief divided by the longest flow path
Soil	soil_ksat_top	Hydraulic Conductivity for topsoil (m/s)	Saturated hydraulic conductivity from 0-30cm depth
	soil_ksat_sub	Hydraulic Conductivity, subsoil (m/s)	Saturated hydraulic conductivity from 30-200cm depth
	soil_sat_wc	Saturated Water Content (m^3/m^3)	Maximum fraction of soil volume that can be occupied by water
	PAWHC	Plant Available Water Holding Capacity (mm)	Maximum depth of soil water that is available for removal by vegetation

750

751 *Table 3. Calibrated parameter values and strength of the correlation (r^2 and mean absolute error, MAE)*
 752 *between calibrated parameters and their estimates from the full regression and reduced regression*
 753 *methods, for the Australian dataset.*

	α_1	α_2	S_{\max} (mm)	d (month^{-1})
Mean and range (calibrated)	0.62	0.74	258	0.66

values)		[0.40; 0.74]	[0.42; 0.80]	[36.5; 500]	[0.10; 1]
Full regression	r^2	0.95	0.96	0.95	0.96
	MAE	0.017	0.022	34	0.10
Reduced regression	r^2	0.20	0.09	0.17	0.06
	MAE	0.038	0.057	86	0.24

754

755 *Table 4. Performance statistics, r^2 and root mean square error (RMSE), for the four model*
 756 *parameterizations for the Australian and US catchments*

	Australia				US			
	Q_{tot}		Q_{min}		Q_{tot}		Q_{min}	
	r^2	RMSE	r^2	RMSE	r^2	RMSE	r^2	RMSE
Calibration	0.98	42.4	0.90	2.4	0.96	108.9	0.88	9.29
Full regression	0.96	47.8	0.84	2.3	0.92	167.5	0.55	9.92
Reduced regression	0.87	88.6	0.53	3.9	0.92	159.3	0.53	9.37
Mean	0.87	89.5	0.55	4.0	0.92	173.2	0.51	9.34

757

758 *Table A1. Parameter levels used in the sensitivity analyses, corresponding to the minimum, 25th, 50th, and*
 759 *75th percentiles, and maximum parameter values.*

Parameter	Min	25th	50th	75th	Max

Smax (mm)	133	200	266	333	399
α_1	0.30	0.45	0.60	0.75	0.90
α_2	0.30	0.45	0.60	0.75	0.90
d	0.33	0.5	0.66	0.83	1.0

760

761 *Table B1. List of basins removed from Newman's dataset (Newman et al., 2015), due to issues with the*
762 *time series. Other basins showed short gaps in the time series but the effect on the long-term average*
763 *was deemed minor. R is the reported average daily runoff in*
764 *basin_annual_hydrometeorology_characteristics_daymet.txt (from Newman et al.'s dataset); P is the*
765 *reported average daily precipitation in basin_annual_hydrometeorology_characteristics_daymet.txt; <q>*
766 *is the calculated average runoff from daily discharge and basin area; <p> is the calculated average*
767 *precipitation from daily precipitation*

Basin	Issue
03 02108000 NE Cape Fear, NC	Area and elevation in basin_characteristics file do not match USGS website or information in gage information file
03 02310947 Withlacoochee River near Cumpressco, FL	Multiple, long, discontinuous gaps in the streamflow record
03 02381600 Fausett Creek near Talking Rock, GA	Calculated average runoff from daily values, <q> is >1.5*reported average daily runoff, R
05 03357350 Plum Creek near Bainbridge, IN	Calculated runoff from daily values, <q>, is less than 50% of reported average daily runoff, R
09 05062500	Calculated average runoff from daily values, <q>

1 2 3 4 5 6 7 8 9 10 11 12 13 14 15 16 17 18 19 20 21 22 23 24 25 26 27 28 29 30 31 32 33 34 35 36 37 38 39 40 41 42 43 44 45 46 47 48 49 50 51 52 53 54 55 56 57 58 59 60	Wild Rice River at Twin Valley, MN	is >1.5*reported average daily runoff, R
	09 05087500	Calculated average runoff from daily values, <q>
	Middle River at Argyle, MN	is >1.5*reported average daily runoff, R
	09 05120500	Calculated runoff from daily values, <q>, is less
	Wintering River near Karlsruhe, ND	than 50% of reported average daily runoff, R
	10 06468250	Calculated runoff from daily values, <q>, is less
	James River near Kensal, ND	than 50% of reported average daily runoff, R
	10 06441500	Multiple long gaps in streamflow record
	11 07067000	Area and elevation in basin_characteristics file do
	Current River at Van Buren, MO	not match USGS website or information in gage
		information file
	12 08079600	Calculated runoff from daily values, <q>, is less
	Brazos River at Justiceburg, TX	than 50% of reported average daily runoff, R
	15 09484000	Multiple extended gaps in streamflow record
	Sabino Creek near Tucson, AZ	throughout
	15 09492400	Calculated average runoff from daily values, <q>
	East Fork White River near Apache, AZ	is >1.5*reported average daily runoff, R
	16 10166430	Calculated runoff from daily values, <q>, is less
	West Canyon Creek near Cedar Fort, UT	than 50% of reported average daily runoff, R
	16 10172700	Calculated runoff from daily values, <q>, is less
	Vernon Creek near Vernon, UT	than 50% of reported average daily runoff, R
	16 10172800	Calculated runoff from daily values, <q>, is less
	South Willow Creek near Grantsville, UT	than 50% of reported average daily runoff, R
	16 10242000	Calculated runoff from daily values, <q>, is less

Coal Creek near Cedar City, UT	than 50% of reported average daily runoff, R
16 10249300 South Twin River nr Round Mountain, NV	Calculated runoff from daily values, $\langle q \rangle$, is less than 50% of reported average daily runoff, R
18 10259200 Deep Creek near Palm Desert, CA	Calculated runoff from daily values, $\langle q \rangle$, is less than 50% of reported average daily runoff, R
18 10263500 Big Rock Creek near Valyermo, CA	Calculated runoff from daily values, $\langle q \rangle$, is less than 50% of reported average daily runoff, R
18 11253310 Cantua Creek near Cantua Creek, CA	Calculated runoff from daily values, $\langle q \rangle$, is less than 50% of reported average daily runoff, R
17 12040500 Queets River nr Clearwater, WA	Runoff ratio is greater than 1; $\langle q \rangle$ is greater than $\langle p \rangle$
17 12041200 Hoh River nr Forks, WA	Runoff ratio is greater than 1; $\langle q \rangle$ is greater than $\langle p \rangle$
17 12056500 NF Skokomish River near Hoodspport, WA	Runoff ratio is greater than 1; $\langle q \rangle$ is greater than $\langle p \rangle$
17 12147500 NF Tolt River near Carnation, WA	Runoff ratio is greater than 1; $\langle q \rangle$ is greater than $\langle p \rangle$ and R is greater than P
17 12147600 SF Tolt River near Index, WA	Runoff ratio greater than 1; R is greater than P
17 12167000 NF Stillaguamish River near Arlington, WA	Runoff ratio greater than 1; $\langle q \rangle$ is greater than $\langle p \rangle$ and R is greater than P
17 12186000 Sauk River near Darrington, WA	Runoff ratio greater than 1; $\langle q \rangle$ is greater than $\langle p \rangle$ and R is greater than P
17 14158500 McKenzie River near Clear Lake, OR	Runoff ratio greater than 1; $\langle q \rangle$ is greater than $\langle p \rangle$

1
2
3
4
5
6
7
8
9
10
11
12
13
14
15
16
17
18
19
20
21
22
23
24
25
26
27
28
29
30
31
32
33
34
35
36
37
38
39
40
41
42
43
44
45
46
47
48
49
50
51
52
53
54
55
56
57
58
59
60

17 14400000	Runoff ratio greater than 1; <q> is greater than
Brookings, OR	<p> and R is greater than P

768

769

770

For Peer Review

771 FIGURES

772 *Figure 1. "Limits" concept used for water partitioning in DWBM. The concept is used to partition both the*
773 *precipitation (P) between wetting (W) and direct runoff, and the wetting between evapotranspiration (ET)*
774 *and storage. The α parameters determine how close the variables are from their limits (dashed lines).*

775

776 *Figure 2. Distribution of the 89 Australian (left) and 641 US (right) catchments used in this study, with*
777 *associated aridity index values. Grey-scale background on the US map delineate the HUC2 regions*
778 *(darker colors represent higher HUC number).*

779

780 *Figure 3. Sensitivity of minimum flow (Q_{min}) to each model parameter. Grey lines represent the relative*
781 *error in parameter values from the regression model (Section 3.1)*

782

783 *Figure 4. Comparison of observed minimum flow Q_{min} , with predictions from the calibrated and mean-*
784 *value parameterizations for Australian catchments. Note that the plot window excludes between 12 and*
785 *16 catchments with high values of Q_{min} . rmse=root mean square error in mm/mo*

786

787 *Figure 5. Comparison of observed minimum flow Q_{min} , with predictions from the calibrated and mean-*
788 *value parameterizations for US catchments. Note that the plot window excludes between 12 and 16*
789 *catchments with high values of Q_{min} . rmse=root mean square error in mm/mo*

790

791

1
2
3 792 *Figure 6. Predictions for Q_{min} (a) and Q_{tot} (b) resulting from a hypothetical land use change – i.e. a change*
4
5 793 *in α_1 and α_2 values – for both the calibrated and the mean-value models. Each point represents one*
6
7 794 *catchment under either 10% (black) or 20% (grey) relative increase or decrease in α_1 and α_2 . All values in*
8
9 795 *the bottom-left quadrant represent an increase in α_1 and α_2 , while all values in the top-right quadrant*
10
11 796 *represent a decrease in the two parameters. Dashed lines represent a 50% difference between the*
12
13 797 *calibrate and mean-value predictions. RMSE for Q_{min} is 0.36 for the “10% change” and 1.2 for “20%*
14
15 798 *change”. For the increase in α_1 and α_2 (bottom-left quadrant), representing afforestation, RMSE for “20%*
16
17 799 *change” is 0.13.*

18
19
20 800

21
22
23 801 *Figure A1. Climate types used in this study: humid continental (Cleveland), subtropical with dry-summer*
24
25 802 *(Nairobi), tropical with dry-winter (San Jose)*

26
27
28 803
29
30
31
32
33
34
35
36
37
38
39
40
41
42
43
44
45
46
47
48
49
50
51
52
53
54
55
56
57
58
59
60

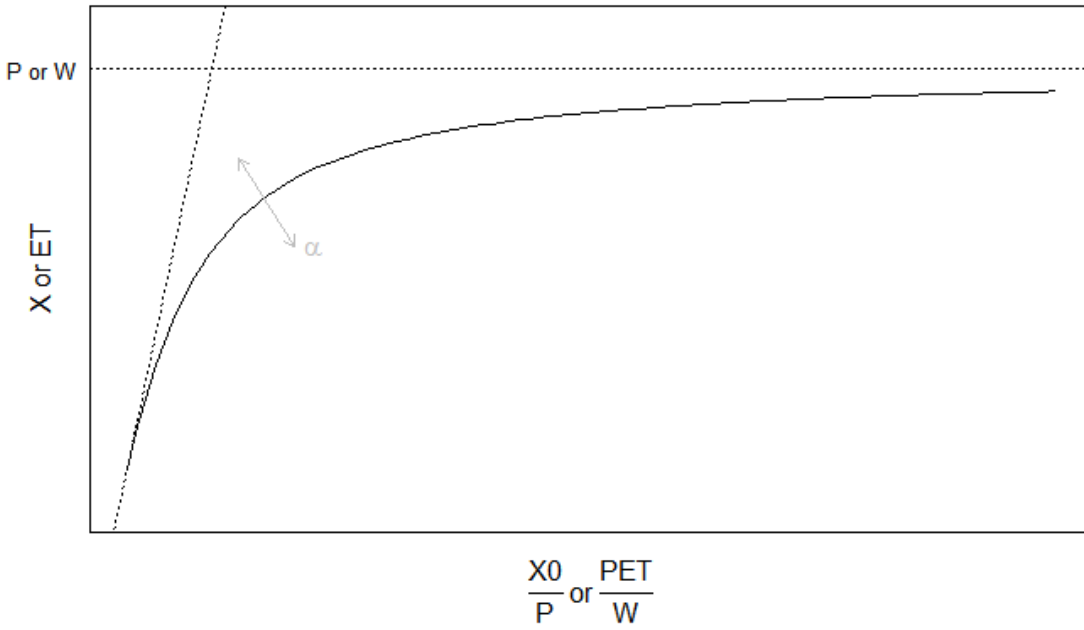


Figure 1. "Limits" concept used for water partitioning in DWBM. The concept is used to partition both the precipitation (P) between wetting (W) and direct runoff, and the wetting between evapotranspiration (ET) and storage. The α parameters determine how close the variables are from their limits (dashed lines).

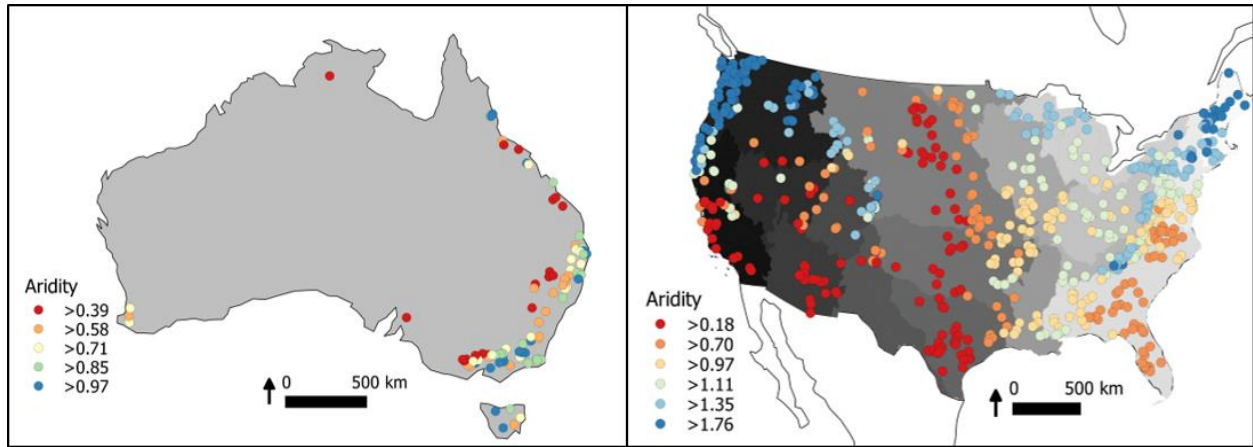


Figure 2. Distribution of the 89 Australian (left) and 641 US (right) catchments used in this study, with associated aridity index values. Grey-scale background on the US map delineate the HUC2 regions (darker colors represent higher HUC number).

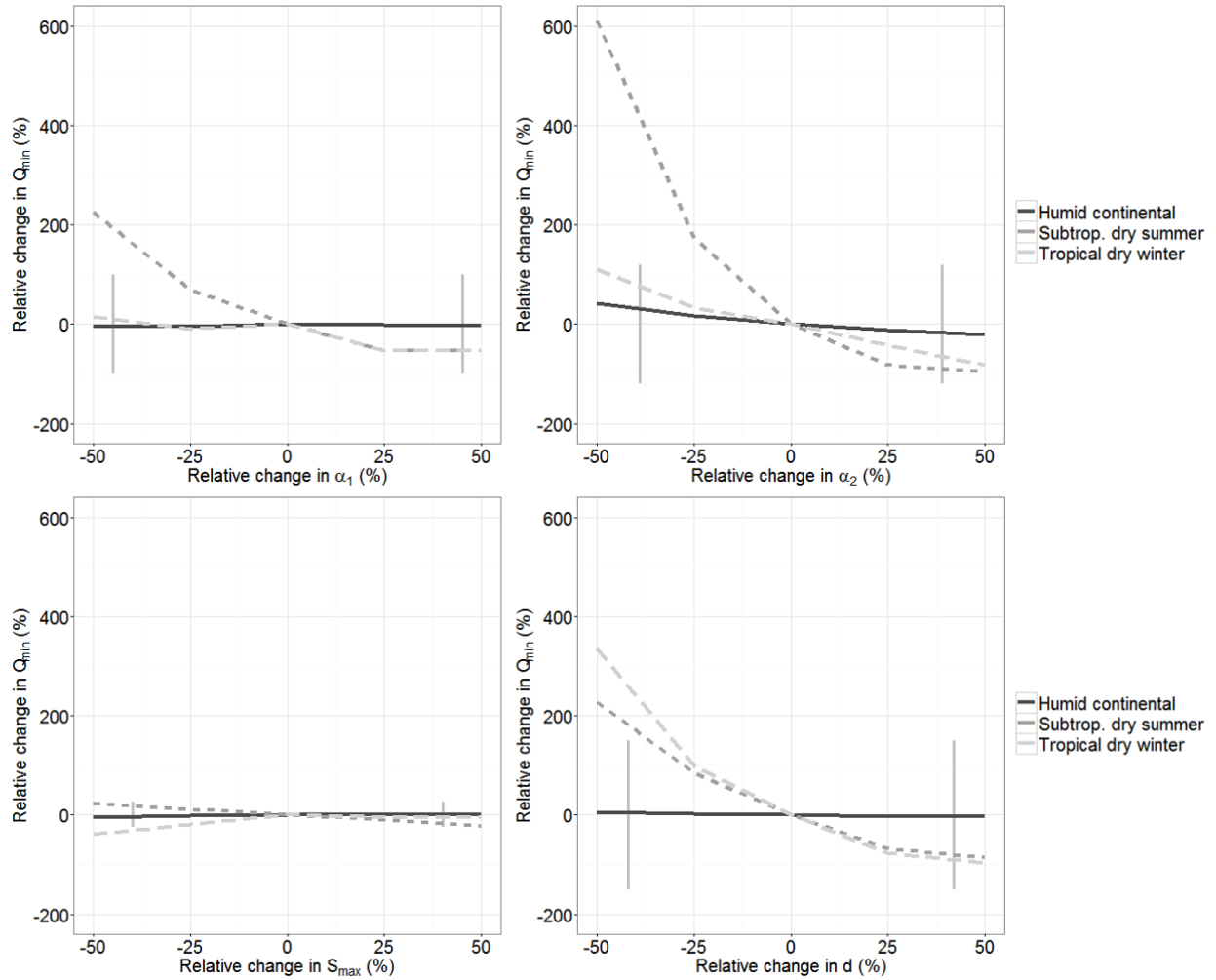


Figure 3. Sensitivity of minimum flow (Q_{min}) to each model parameter. Grey lines represent the relative error in parameter values from the regression model (Section 3.1)

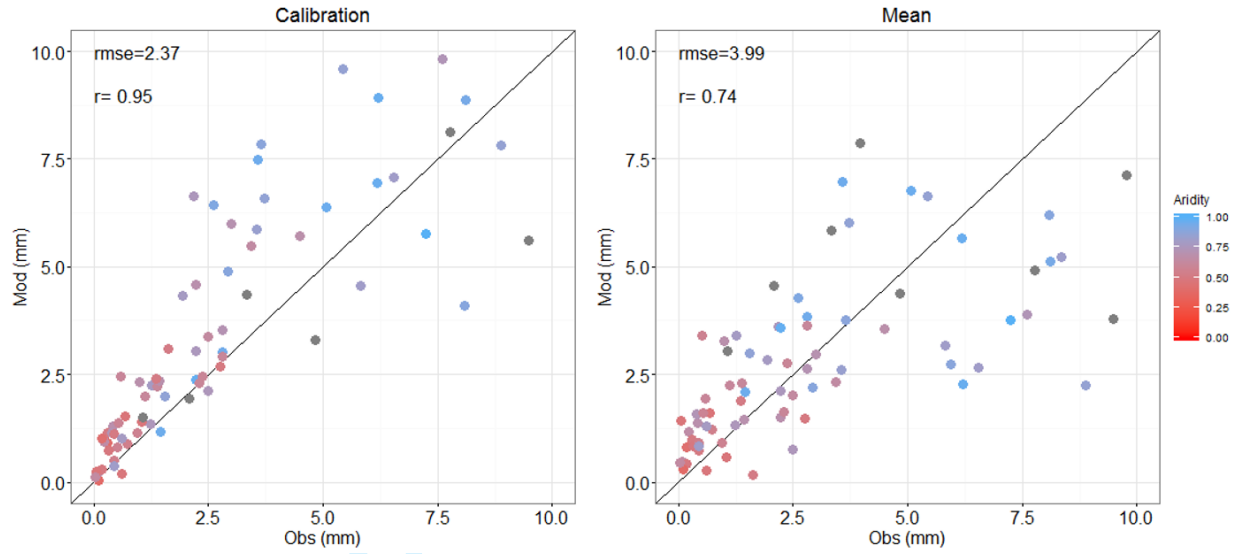


Figure 4. Comparison of observed minimum flow Q_{min} , with predictions from the calibrated and mean-value parameterizations for Australian catchments. Note that the plot window excludes between 12 and 16 catchments with high values of Q_{min} . $rmse$ =root mean square error in mm/mo

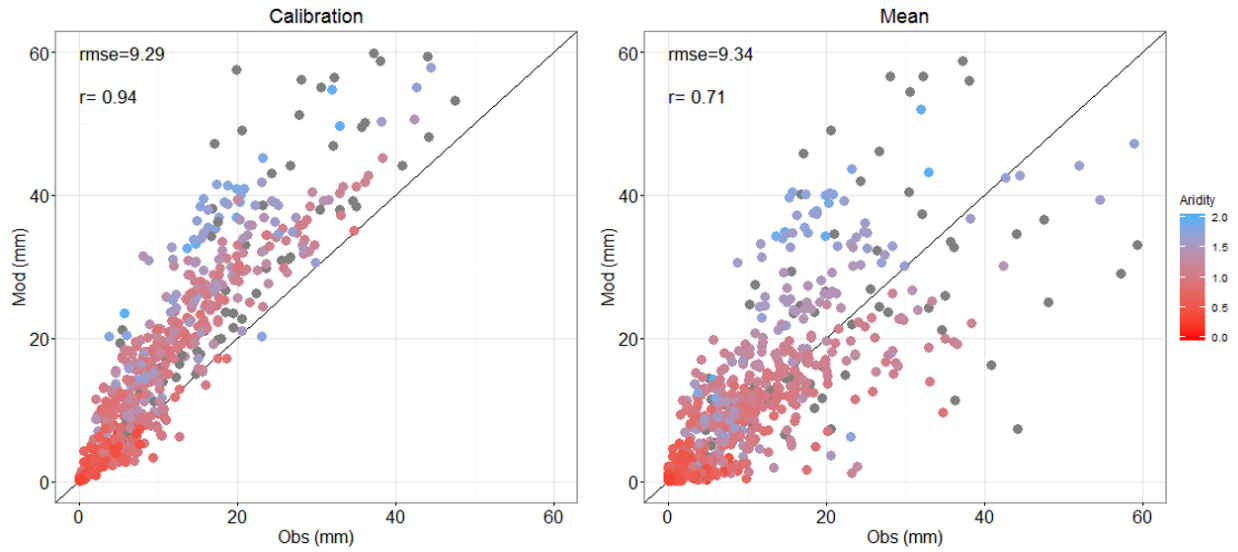


Figure 5. Comparison of observed minimum flow Q_{min} , with predictions from the calibrated and mean-value parameterizations for US catchments. Note that the plot window excludes between 12 and 16 catchments with high values of Q_{min} . $rmse$ =root mean square error in mm/mo

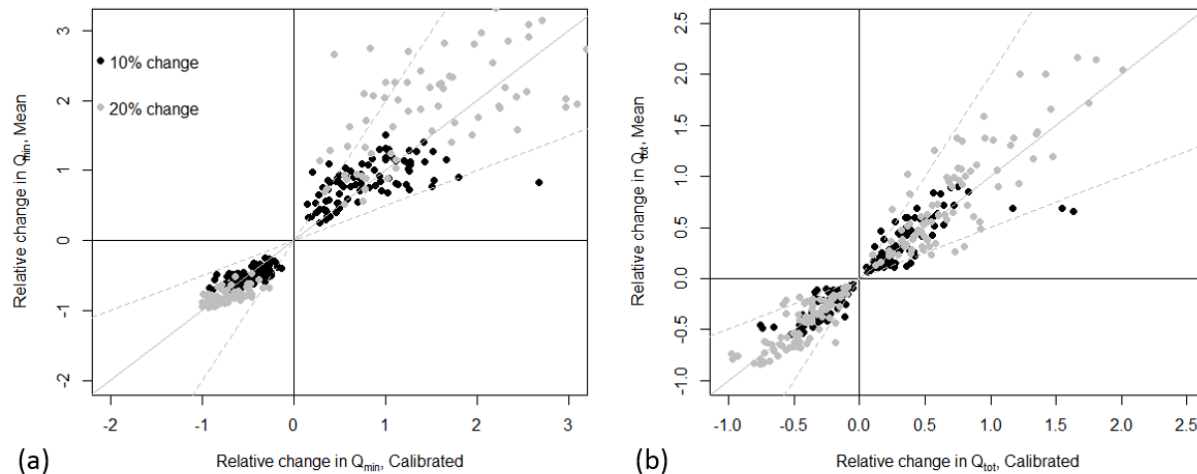


Figure 6. Predictions for Q_{min} (a) and Q_{tot} (b) resulting from a hypothetical land use change – i.e. a change in α_1 and α_2 values – for both the calibrated and the mean-value models. Each point represents one catchment under either 10% (black) or 20% (grey) relative increase or decrease in α_1 and α_2 . All values in the bottom-left quadrant represent an increase in α_1 and α_2 , while all values in the top-right quadrant represent a decrease in the two parameters. Dashed lines represent a 50% difference between the calibrate and mean-value predictions. RMSE for Q_{min} is 0.36 for the “10% change” and 1.2 for “20% change”. For the increase in α_1 and α_2 (bottom-left quadrant), representing afforestation, RMSE for “20% change” is 0.13.

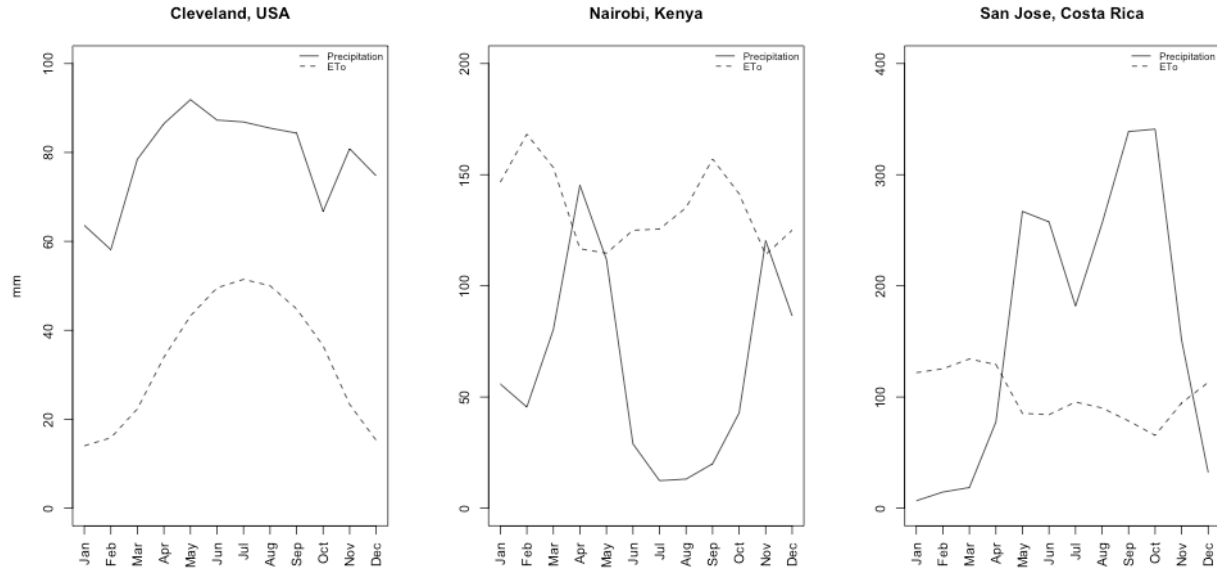


Figure A1. Climate types used in this study: humid continental (Cleveland), subtropical with dry-summer (Nairobi), tropical with dry-winter (San Jose)